Advances in Geo-Energy Research

Vol. 5, No. 2, p. 222-232, 2021

Original article

# Water invasion performance of complex fracture-vuggy gas reservoirs based on classification modeling

Xiaobing Han[1], Xiaohua Tan[1]*, Xiaoping Li[1], Yu Pang[2], Liehui Zhang[1]

[1]*State Key Laboratory of Oil and Gas Reservoir Geology and Exploitation, Southwest Petroleum University, Chengdu 610500, P. R. China*
[2]*Department of Chemical and Petroleum Engineering, University of Calgary, Calgary T2N 1N4, Canada*

**Keywords:**
Fractured-vuggy gas reservoir
discrete fracture network
distribution classification
water invasion

**Cited as:**
Han, X., Tan, X., Li, X., Pang, Y., Zhang, L. Water invasion performance of complex fracture-vuggy gas reservoirs based on classification modeling. Advances in Geo-Energy Research, 2021, 5(2): 222-232, doi: 10.46690/ager.2021.02.11

**Abstract:**
The complexity of the pore structure, spatial development, fractures, and pore distribution of fractured-vuggy carbonate reservoirs influences the water invasion dynamics of gas reservoirs, which is crucial in the dynamic research of strongly heterogeneous reservoirs. In this study, the collocation relationship of pore-vuggy fractures is described by the quantitative characterization of their attribute parameters. The discrete fracture network model is used to match and construct the fractures in different modes. The distribution classification method is used to model three-dimensional geological reservoirs in terms of their geometric and attribute characteristics. Bottom-water and edge-water gas reservoirs are constructed separately using numerical simulation, and the dynamic characteristics of water invasion are described. The results show that the proposed method is suitable for the geological modeling of fractured-vuggy gas reservoirs with strong heterogeneity and complexity. The modeling accuracy is improved because the gas reservoir heterogeneity and water invasion's dynamic characteristics can be described accurately. Six stages of water invasion are identified from the numerical simulation of water invasion. This method provides theoretical guidance for the study of heterogeneous gas reservoirs with water.

## 1. Introduction

Fractured-vuggy gas reservoirs feature three types of reservoir spaces, namely, pore, vuggy, and fracture spaces, and present unique triple-medium characteristics. The porosity, permeability, and distribution characteristics of different reservoir spaces can vary significantly; this means that effective reservoirs commonly demonstrate strong formational heterogeneity and extremely complex distributions. Accordingly, the quantitative evaluation of this type of reservoir and establishing an appropriate three-dimensional (3D) model are popular research topics (Golparvar et al., 2018; Fan et al., 2019; Wang et al., 2020).

During the development of gas reservoirs, the formation pressure inside the gas reservoir decreases with natural gas extraction. The resulting drop in pressure gradually spreads elastically to the outer natural water causing the elastic expansion of formation water and reservoir rock in the natural water area. The impacts of fracture and seepage on the pore heterogeneities of highly volatile bituminous coal and water invasion degree have rarely been characterized quantitatively. To address this, Li et al. (2019) established relationships between water invasion degree and the fracture-seepage pore heterogeneities of highly volatile bituminous coal. Presently, simulating water invasion in fractured-vuggy gas reservoirs using known fracture models, such as the double-porosity, single-permeability, and double-porosity/double-permeability models, is challenging.

Reports on the methods for modeling fractured-vuggy reservoirs are available (Samir et al., 2012; Fan et al., 2019; Xu et al., 2020; Zhou et al., 2020). Conventional double-hole gas reservoir simulation systems cannot simulate the seepage mechanism of fractured-vuggy reservoirs (Kossack et al., 2006). Kossack et al. (2006) numerically simulated a two-hole reservoir to establish a composite curve (i.e., a phase permeability curve and a capillary pressure curve) to simulate the oil recovery effect of fractured-vuggy gas reservoirs. Wu et al. (2011) proposed a multiple-continuum conceptual model based on geological data and observations of core samples

Yandy Scientific Press

*Corresponding author.
*E-mail address*: 202011000127@stu.swpu.edu.cn (X. Han); xiaohua-tan@163.com (X. Tan); lixiaoping@swpu.edu.cn (X. Li); yupang0317@gmail.com (Y. Pang); zhangliehui@vip.163.com (L. Zhang).

Received March 25, 2021; revised April 12, 2021; accepted April 13, 2021; available online April 16, 2021.

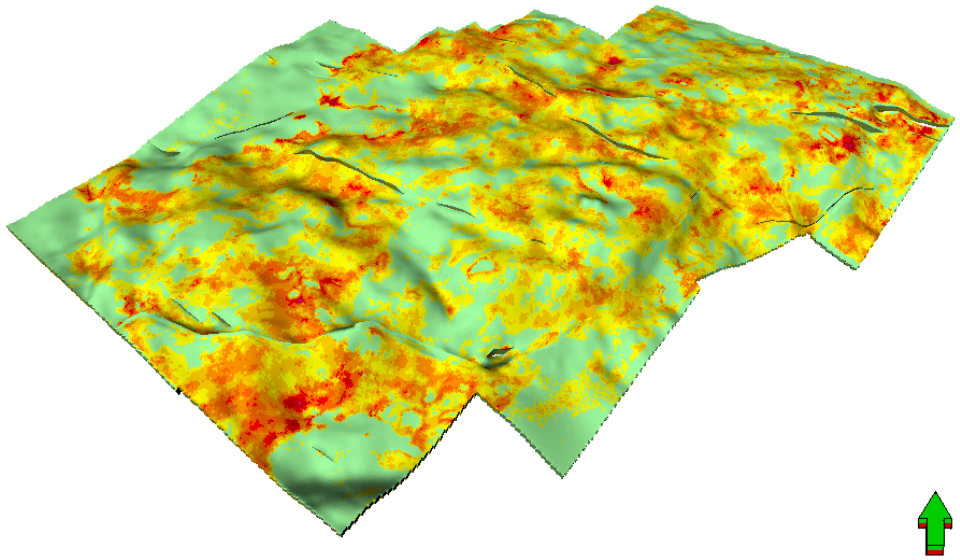

**Fig. 1.** Structure of the Longwangmiao Formation gas reservoir block.

from carbonate formations to study single and multiphase flow behavior in fractured-vuggy reservoirs. Using physical experiments and numerical simulation methods, Lyu et al. (2017) applied an approach that combined fractures and cavities in the reservoir to establish an indoor multiscale physical model of complex fracture structures that could produce results similar to those obtained under actual reservoir conditions. Gomes et al. (2004) summarized the experiences and recommendations of several experts in the static simulation of complex fractured-vuggy reservoirs. There are many reservoirs connected to external natural waters in Sichuan. Some have a large volume of natural water with sufficient energy; in these cases, the water invasion phenomenon significantly impacts development (Li et al., 2019). Espinola-Gonzalez et al. (2016) established a numerical simulation model of water invasion in conventional sandstone gas reservoirs and designed a relevant development scheme according to the characteristics of water invasion.

However, in gas fields in Sichuan, China, nearly all active water-intrusion occurs aside fractures because of the complex geological conditions of the area. Zhang et al. (2005) established a nonlinear coupled fluid simulation model suitable for bottom-water gas field development considering a nonlinear flow field and the matrix within fractures. Dynamic research on triple-medium carbonate reservoir water invasion, among other methods, is often based on experiments and core analyses. Many scholars have constructed physical models of vugs and fractures through experiments to characterize the influence of triple media on water invasion; some researchers even analyzed the cores of different types of reservoirs and the influence of water invasion in terms of phase permeability (Yuan et al., 2014; Ni et al., 2016; Li et al. 2019; Wang et al., 2019a).

However, none of the above methods can realize the macroscopic analysis of water invasion in a complete fracture-cavity gas reservoir because the numerical simulation software presently available supports only reservoir simulations with dual media (Akbarifard et al., 2020). In this paper, a fractured-vuggy reservoir geological model is constructed using a systematic classification and multitype fusion method by establishing the attribute collocation relationship between pores, voids, and fractures in the microspace of the reservoir. Discrete fracture network (DFN) model construction and improved traditional modeling methods are used to establish classification models for different pore, vuggy, and natural fracture reservoirs. Finally, a numerical simulation model of water invasion in complex fractured-vuggy gas reservoirs is constructed to describe the dynamic characteristics of the invasion of bottom and edge waters understand the water invasion mechanism better.

## 2. Field description

The Longwangmiao Formation gas reservoir lies at a depth of approximately 4,700 m; its formation thickness is approximately 80 m with local high-point characteristics; and it is a general fractured-vuggy type. The development degree of fractures and cavities in different blocks on the plane and at different vertical intervals is uneven (Fig. 1). Local fracture-pore and pore-type reservoirs belonging to low-porosity and medium/high-permeability gas reservoirs occur in the area. The original formation pressure of the gas reservoir is 75.83 MPa, the pressure coefficient is 1.64, and the formation temperature is 140.21 °C. Thus, the reservoir of interest is a high-temperature/high-pressure gas reservoir. The main body of the reservoir has a uniform gas-water interface and an elevation of −4,385 m. Thus, the reservoir is a lithologically structured gas reservoir with edge water. The dip angles of the fractures are primarily in the range of 0-15° and 70-90°, and the main angles are high-angle structural fractures (45-90°), including filled and unfilled high-angle fractures. Horizontal fractures (< 15°), low-angle skew joint fractures, and filled high-angle joint fractures are formed earlier and accompanied by large-scale solution expansion holes. The fracture strike direction is

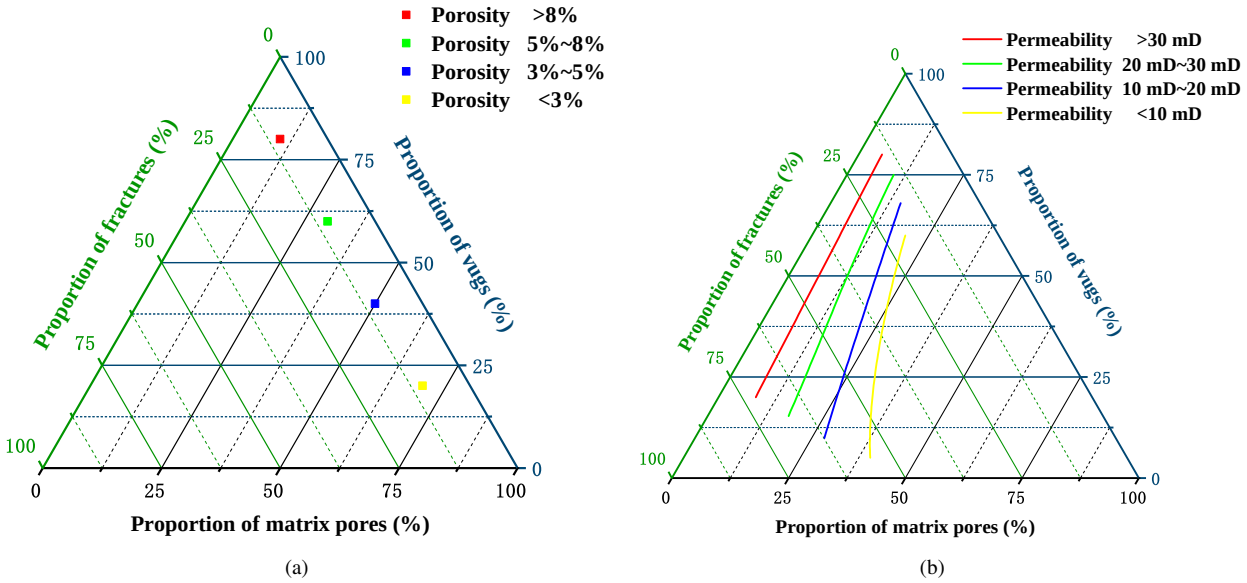


**Fig. 2.** Ternary diagram of attributes with different proportions of pore-vug-fracture reservoir spaces.

mainly northwest-west (NWW) (Wang et al., 2019b).

## 3. Collocation relation of pore-vuggy-fractures property parameters

Core analysis is required to collocate fractured-vuggy gas reservoir property parameters and establish the pore-vuggy-fractured properties' collocation in the reservoir's microscopic space. Furthermore, the microscopic structure of the reservoir must be clarified and microscopic seepage process must be reduced to achieve a precise description of reservoir space and seepage channel. These procedures will help obtain a clear quantitative pore-vuggy-fracture image of the reservoir space.

The distributions of porosity and permeability in different media reflect the main collocations of attribute parameters in this paper. The matrix porosity was 2-3%, vug porosity was 2-8%, and fracture porosity was 0-1%. In this case, all pores were normally distributed. Moreover, the matrix pore permeability was 0-0.1 mD, vug permeability was 0-45 mD, and fracture permeability was 0-50 mD. As in the previous case, the permeability of the different media was normally distributed.

The porosity and permeability in different proportions of the reservoir space were determined for the fractured-vuggy gas reservoir model as shown in Fig. 2.

## 4. Construction of distribution and classification models

The distribution and development rules for different reservoirs were based on the identification and descriptions of gas reservoir units using stochastic modeling; the matrix pores, vugs, and fracture models were individually established.

The geological model was simulated by a 1100×1100 $m^2$ square control unit. The step size of the grid in the X and Y directions was set to 10 m. Assuming a reservoir thickness of 40 m, the grid was divided into 4 longitudinal layers, and 10

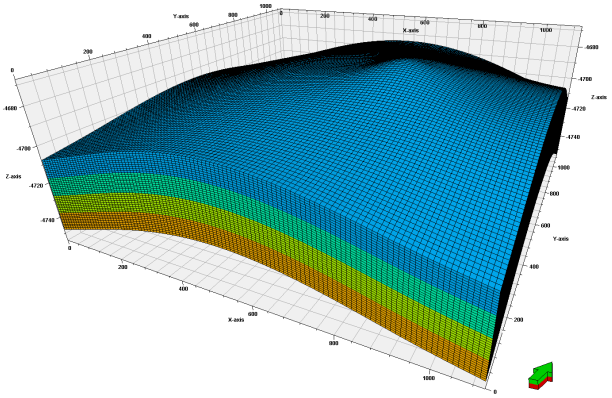

**Fig. 3.** Grid construction of geological model for a fractured-vuggy gas reservoir.

longitudinal grids were set in each layer. The total mesh number of the model was 110 × 110 × 40 = 484,000. Given the gentle structure and multiple high points of the Longwangmiao Formation, an anticlinal structural gas reservoir was established in the structural high point of the eastern region. Fig. 3 shows the geological model of this reservoir.

### *4.1 Pore-vuggy reservoir modeling*

Because the reservoir is block-like, vertically continuous, and superposed within the plane, the variation function was first obtained using well-point data. The theoretical variation function was then obtained by fitting with the experimental variation function, i.e., the theoretical model of the variation function. The variation function is an important parameter in stochastic simulations and is defined as the variance of the difference between the values of the regionalized variable $Z(x)$ at points $x$ and $x+h$. The relevant formula is:

$$r(h) = \frac{1}{2}E[Z(x+h) - Z(x)]^2 \quad (1)$$

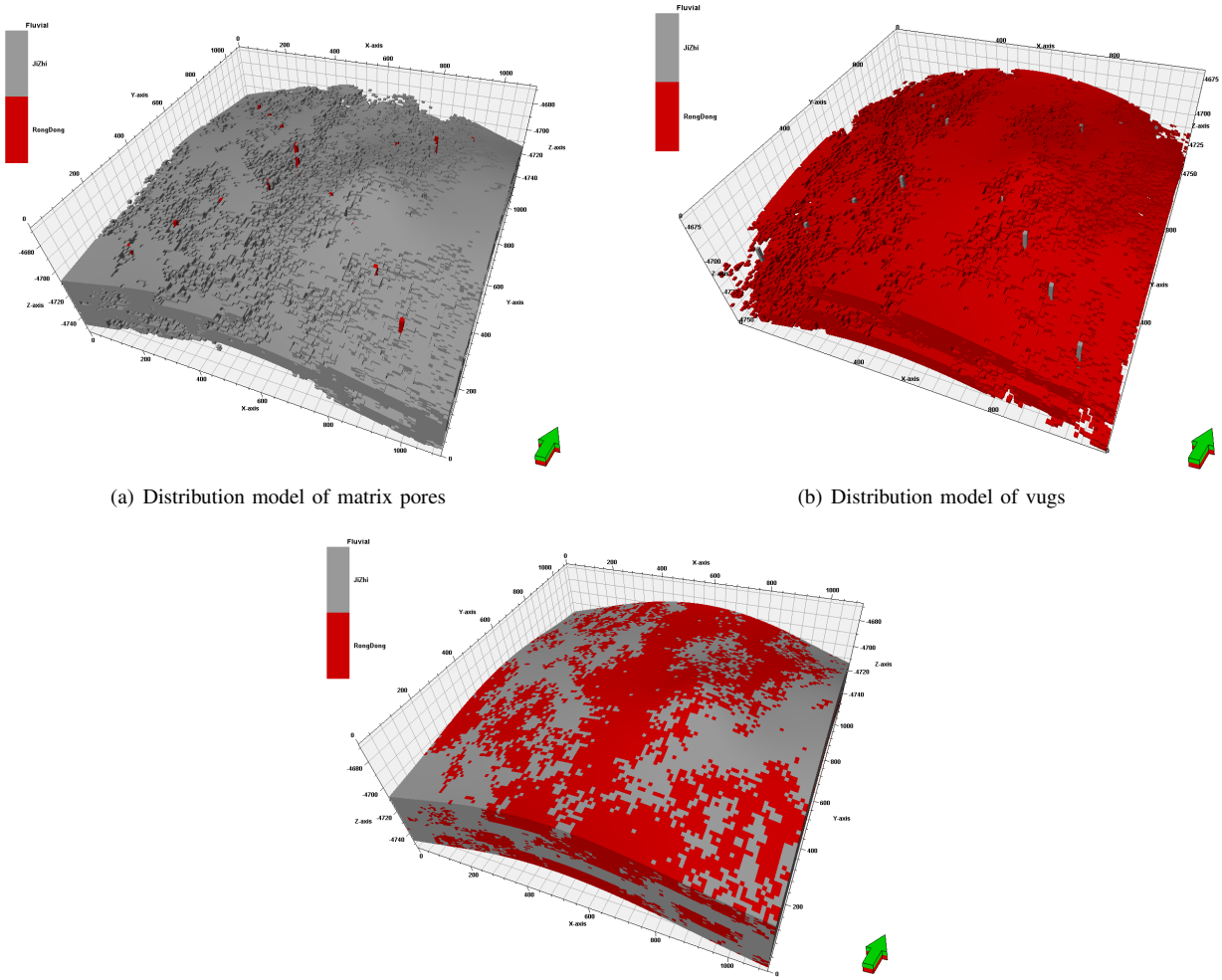


(a) Distribution model of matrix pores

(b) Distribution model of vugs

(c) Distribution model of the pore-vuggy reservoir

**Fig. 4.** Modeling results of the pore-vuggy reservoir.

The variation function includes three main eigenvalues, i.e., range, fund station, and nugget. These three characteristic values reflect the spatial variation characteristics of the reservoir parameters. A spherical variation function model was used in the 3D geological modeling of the area, and the data of each layer and rock faces were individually analyzed. During variation function fitting, the nugget constant was 0, and the base station value was less than but close to 1. Analysis of the fit of the experimental variation function model with known points revealed that the main range of this region was 700 m; the secondary range was 500 m. The primary and secondary ranges of different layers and phases varied slightly but fluctuated similarly around this value. The sequential indicator simulation method was used when conducting the phase modeling analysis (Fig. 4).

## *4.2 DFN modeling*

Because discrete fractures are the main flow channels in fractured-vuggy gas reservoirs, accurate characterization of natural fractures is an important aspect of modeling this type of gas reservoir.

The bottom layer of the Longwangmiao Formation experienced three major tectonic movements, i.e., Caledonian Taconic movement at the end of the Ordovician, Indo-Chinese movement, second act Himalayan movement, and third act Himalayan movement. Furthermore, the tectonic fractures of the formation in the Moxi block are relatively well-developed because of the influence of multistage tectonic movements. The dip angles of the fractures are mainly in the range of 0-15° and 70-90° (Fig. 6); the high-angle structural fractures are approximately 45-90°, and the horizontal fractures are $<$ 15°. The development degree of low angle oblique fractures is weak, and the fracture strike is mainly in the NWW direction (Fig. 5) (Yuan et al., 2014).

When DFN was constrained, 308 fractures were automatically detected through random modeling. Among these fractures, 111 were high-angle structural fractures in the NWW direction, as shown in Fig. 7(a), and 107 were high-angle structural fractures in the NE direction, as shown in Fig. 7(b); 54 were horizontal fractures in the NWW direction, as shown in Fig. 7(c); 36 were horizontal fractures in the NE direction, as shown in Fig. 7(d). Table 1 shows the DFN statistical parameters.

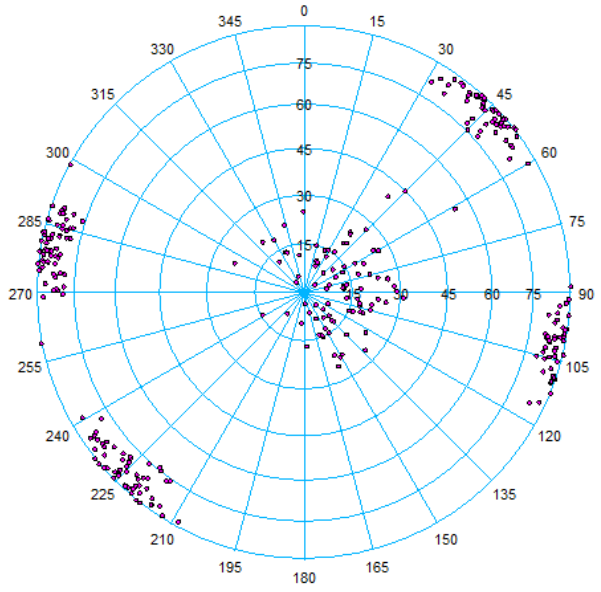


**Fig. 5.** Rose map of natural fractures.

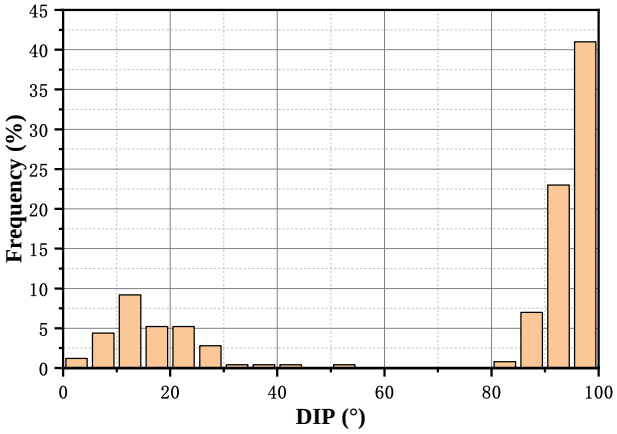


**Fig. 6.** Dip distribution of natural fractures.

## 5. Property modeling of the fractured-vuggy gas reservoir

Fusion of attribute parameter model mainly adopted a distribution model under the restriction of parameter integration method. The cave reservoir, owing to no overlap in the grid, can integrate directly. Fracture network porosity can be treated according to fracture porosity requirements, directly added to the mesh.

### 5.1 Modeling the properties of the pore-vuggy reservoir

The sequential Gaussian simulation random algorithm was adopted to establish the corresponding attribute parameter models for pore-vuggy reservoirs. During the simulation of different reservoir types, the main range direction, main range value, secondary range value, and the vertical range value fitted by the variation function of different reservoir types were individually established. The simulation process conformed to the heterogeneity of vuggy distribution as follows: (1) the data were processed, changed according to the normal distribution, ensuring that the reservoir parameter data conformed to the Gaussian distribution; (2) the variation function was fitted to the vuggy reservoir property model; (3) a distribution model of the vuggy reservoir was constructed to include a phase-controlled constraint; (4) sequential Gaussian simulation was adopted to establish the pore-vuggy reservoir porosity model. The simulation process for the permeability of the pore-vuggy reservoir was identical, and the simulation results are shown in Figs. 8 and 9.

### 5.2 Modeling of fracture properties

The fracture mesh properties were calculated, and the fracture model was transformed into fracture properties in the double-porosity/double-permeability model. The main parameters included fracture porosity, fracture permeability, and the sigma parameter, which described the connectivity between the matrix and the fracture. The equivalent parameter calculation method, described by Eq. (2), was adopted to establish the fracture porosity model, as shown in Fig. 10. Good connectivity between the matrix and fracture was observed. Sigma was set as 1 (Fig. 11). Golder technology and ODA data statistics were used to calculate the equivalent permeability of fractures in three directions, based on the total area of the fracture in a single grid and the different parameters of the fracture, as shown in Fig. 12.

Eq. (2) is given as follows:

$$\varphi_f = \frac{A_f e_f}{V_{cell}} \times 100 \tag{2}$$

where $\varphi_f$ is the mesh fracture porosity (%); $A_f$ is the fracture area within the mesh ($m^2$); and $e_f$ is the fracture opening in the mesh (m).

**Table 1.** Discrete fracture network statistical parameters.

| Direction | Fracture type | Fracture number (-) | Angle (°) |
|---|---|---|---|
| NWW | High-angle structural fracture | 111 | 70-90 |
| NE | | 107 | |
| NWW | Horizontal fracture | 54 | 0-15 |
| NE | | 36 | |

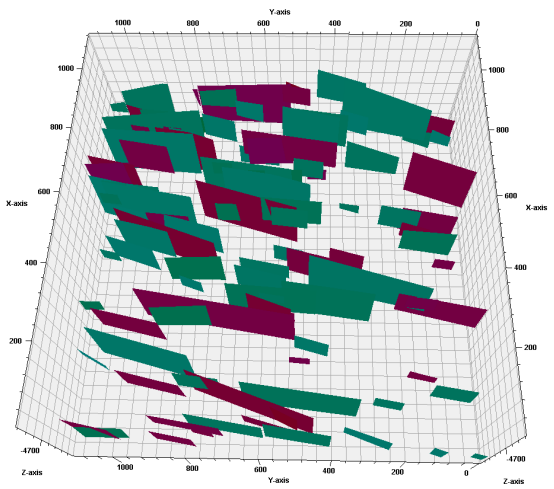


(a) The NWW high-angle structural fracture system

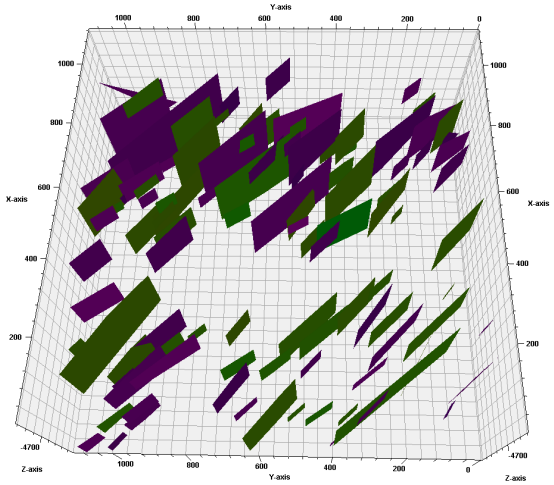


(b) The NE high-angle structural fracture system

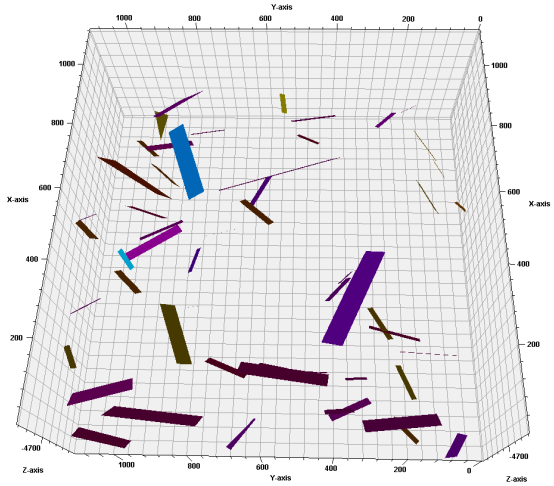


(c) The NWW horizontal fracture system

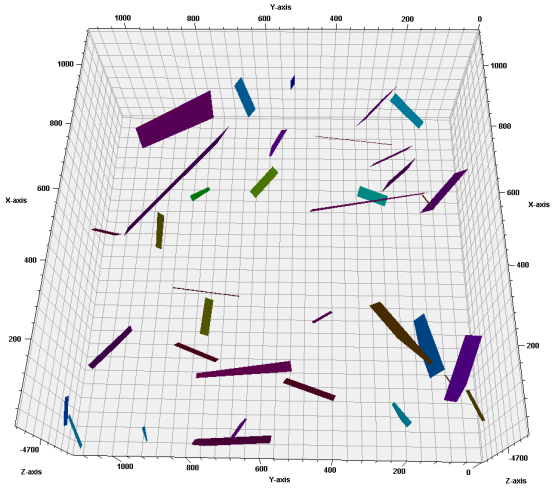


(d) The NE horizontal fracture system

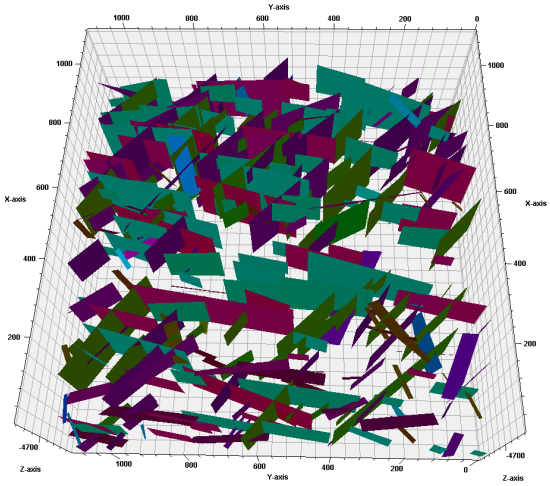


(e) The complete distribution of natural fractures

**Fig. 7.** Natural fracture distribution model.

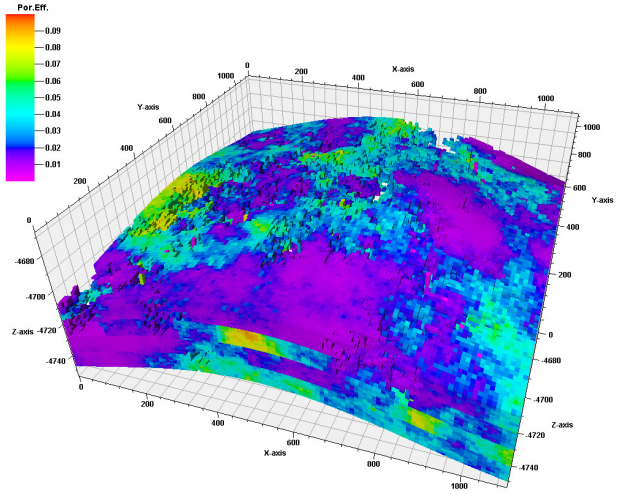


(a) Matrix pore porosity model

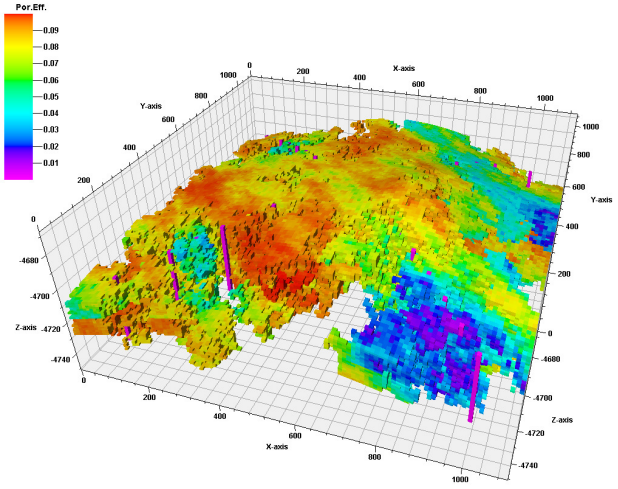


(b) Vug porosity model

**Fig. 8.** Porosity model of the pore-vuggy reservoir.

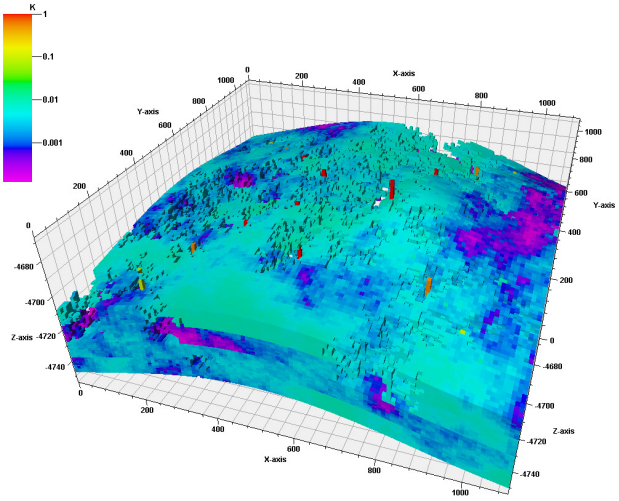


(a) Matrix pore permeability model

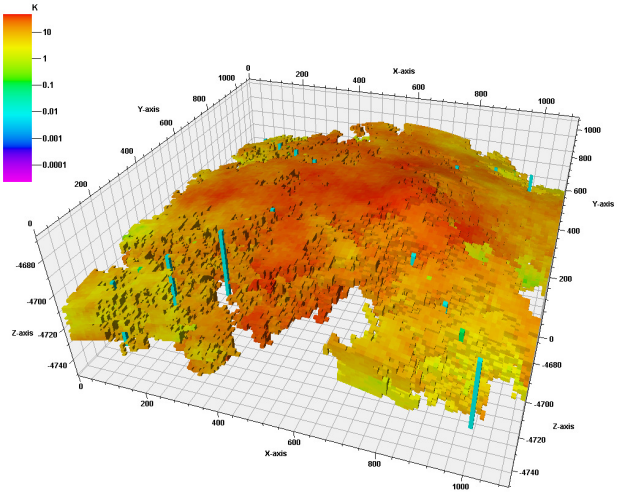


(b) Vug permeability model

**Fig. 9.** Permeability model of the pore-vuggy reservoir.

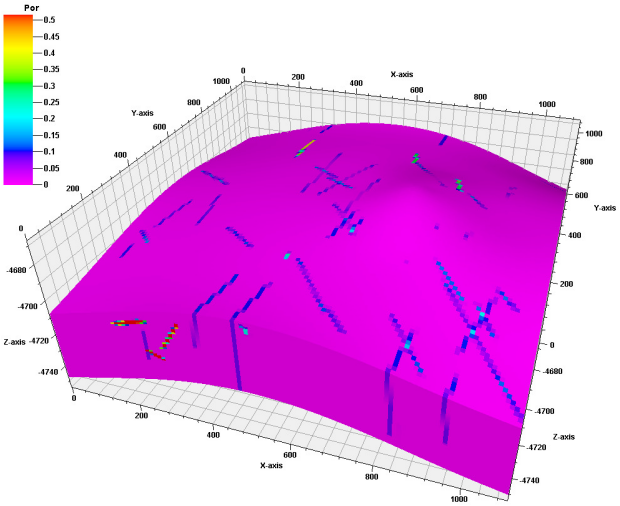


**Fig. 10.** Porosity model of fractures.

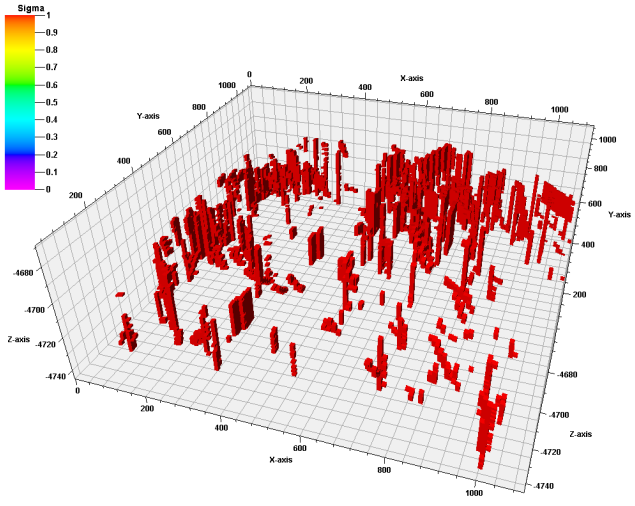


**Fig. 11.** Sigma model of fractures.

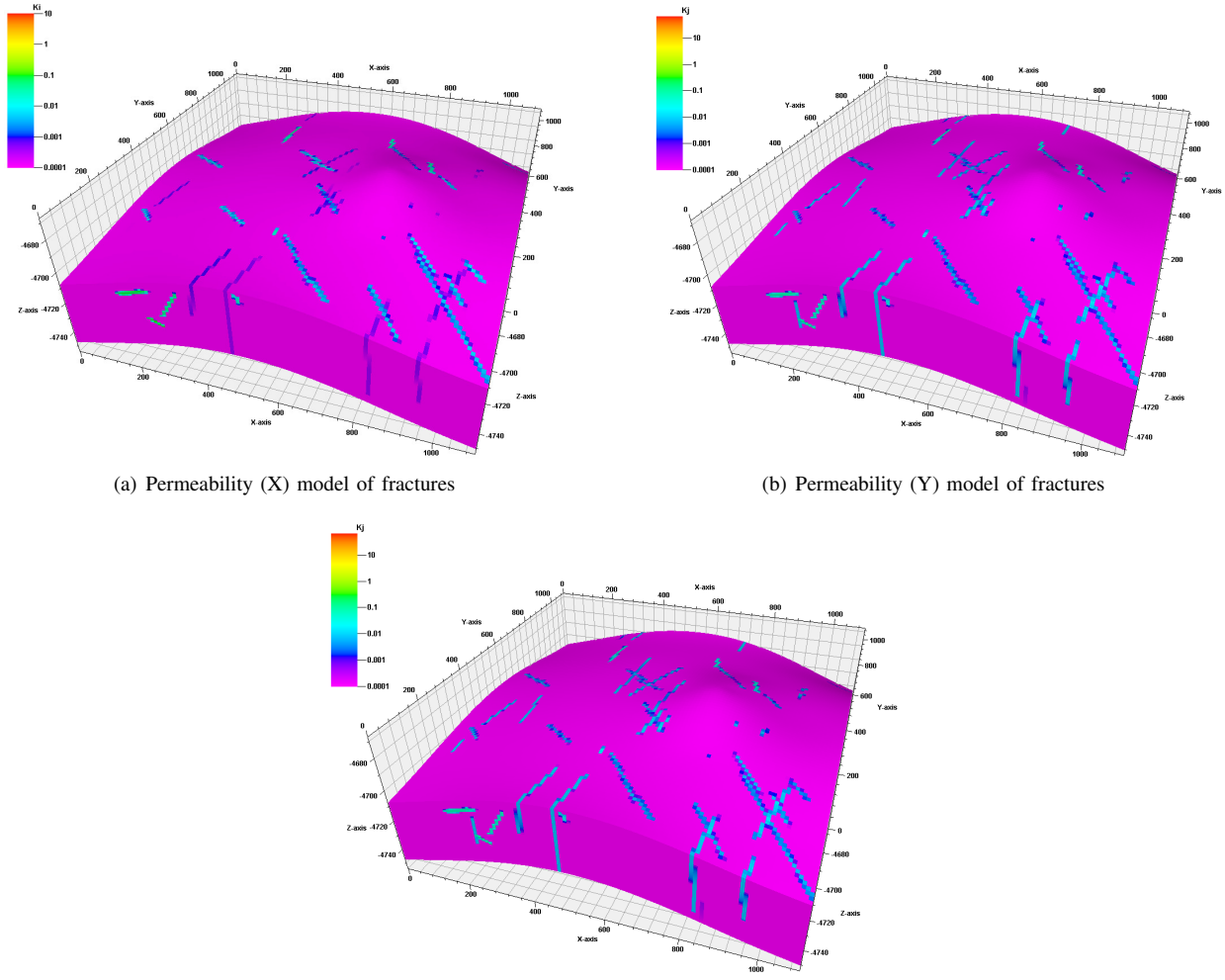


(a) Permeability (X) model of fractures

(b) Permeability (Y) model of fractures

(c) Permeability (Z) model of fractures

**Fig. 12.** Fracture permeability models.

## 6. Relative permeability curve

The relative permeability curve describes the relationship between relative permeability and wet-phase fluid saturation. The condition of a gas reservoir is complex and variable, and relative permeability is not the only function of saturation. Therefore, the interaction of fluid in pore-vuggy reservoirs and the natural fracture system may exhibit considerable variations. As such, the phase permeability data should be established separately; specifically, individual datasets for the pore-cavity (Fig. 13) and fracture system (Fig. 14) should be constructed.

## 7. Dynamic characteristics of water invasion

The water invasion's dynamic characteristics were studied based on the model established above. Accurate numerical simulation results of water invasion in gas reservoirs are often challenging to obtain for two reasons. First, accurate descriptions of fractures in conventional single-porosity media models are difficult to achieve. Second, even if a dual-porosity medium model is adopted, the conventional model's grid size is generally rough. Thus, fine details of the heterogeneous characteristics of fracture distributions and, accordingly, the phenomenon of fracture water channeling cannot be described accurately. In this study, the heterogeneous distribution of fractured-vuggy reservoirs was realized based on the construction of a systematic classification model of these reservoirs. The grid around the well was infused by the near-well module (NWM) in a simulator, thus, enabling the entire process of water invasion to be demonstrated realistically.

The water invasion characteristics of gas reservoirs with water were established by setting the bottom and edge waters, and the water invasion dynamic characteristics were subsequently analyzed.

### *7.1 Bottom-water invasion*

A gas-water interface was established 4,728 m below the bottom of the reservoir to simulate the coning phenomenon of bottom water in fractured-vuggy gas reservoirs. Here, the water body size was set to $3.452 \times 10^5$ $m^3$, the compression coefficient of water is 0.001 $bar^{-1}$, and the production index was 20 $m^3/day/bar$.

The bottom-water invasion of the fractured-vuggy gas reservoir was simulated by adopting a grid around the infill

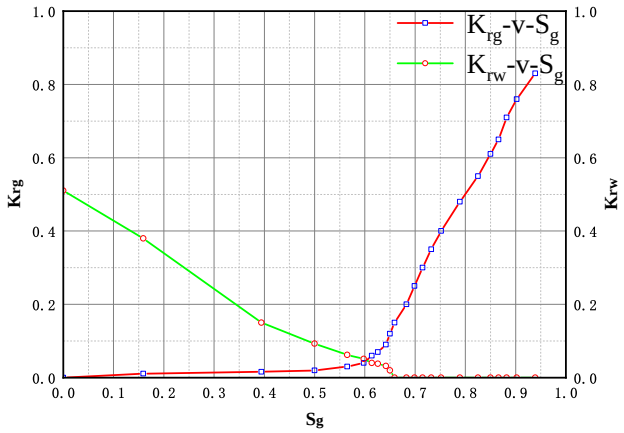


**Fig. 13.** Gas-water permeability curve of the pore-vuggy system.

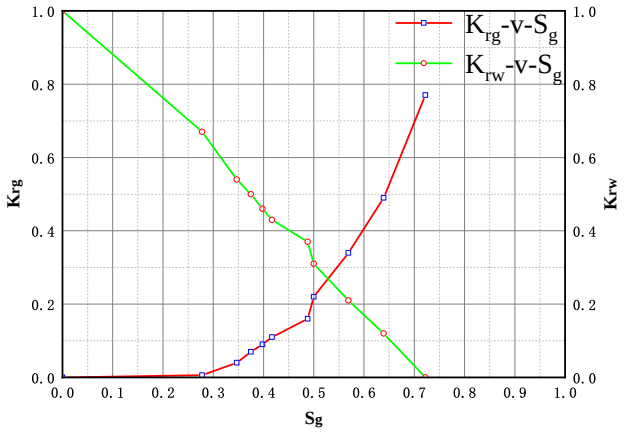


**Fig. 14.** Gas-water permeability curve of the fracture system.

well using the NWM. The $7 \times 7 \times 8$ grid around the test well was infilled four times horizontally and two times vertically to obtain a $28 \times 28 \times 16$ grid system. This expanded system allowed for the finer delineation of the dynamic characteristics of water invasion in the reservoir (Fig. 15).

## 7.2 Edge-water invasion

The edge-water invasion phenomenon in fractured-vuggy gas reservoirs was simulated by setting the gas-water interface at 297 m from the northern boundary. The edge-water body in the north was $1.541 \times 10^7$ $m^3$, the water compression coefficient was 0.01 $bar^{-1}$, and the production index was 20 $m^3/day/bar$.

The simulation of edge-water invasion was conducted. The initial water saturation and change in water saturation predicted by the model at the end of the simulation indicated that the systematic classification model of pore-vuggy-fracture reservoirs provided a good simulation of the complete edge-water invasion process.

Simulation of the water invasion process indicated that fractures were the main channels of fluid flow. The water breaking time of the gas well was closely related to the distribution of fractures. These findings were consistent with actual observations.

The variation of saturation in the study area was divided into several stages according to the dynamic change characteristics of water influx over time. Figs. 16 and 17 illustrate the six stages of edge-water invasion.

**Stage 1: Initial stage**

In the initial stage of water invasion, an obvious gas-water boundary with static characteristics may be observed.

**Stage 2: Initial water invasion**

As the production of a single well begins, the formation pressure around the well decreases. When the pressure drop of a single well spreads to the gas-water boundary, intrusion of the side water begins to occur because of the pressure difference.

**Stage 3: End of the initial water invasion**

The edge water mainly flows side fractures with high permeability and into the highly porous reservoirs.

**Stage 4: Initiation of water retreat**

As the water penetrates the bottom wellbore, a single well begins to produce water, leading to reduced water drive pressure. The formation pressure of the residual gas in the lower part of the well is greater than the water drive pressure in the upper part of the horizontal dividing line of the well. Water retreat occurs in the vuggy reservoir with large pores, and the gas in the upper part of the formation begins to "bite" the water invasion part.

**Stage 5: End of water retreat (initiation of secondary water invasion)**

In the water retreat stage, the formation pressure in the lower part of the well gradually decreases with the continuous recovery of the residual gas. When the water drive pressure at the upper part of the well is reduced, secondary water invasion occurs.

**Stage 6: End of secondary water invasion**

During secondary water invasion, water mainly flows side the fractures, and the gas saturation of the vuggy reservoir markedly decreases.

## 8. Conclusions

A systematic classification and multitype fusion method for establishing a water invasion model suitable for describing fractured-vuggy gas reservoirs in the Longwangmiao Formation was proposed in this study. The dynamic characteristics of water invasion in this reservoir were carefully analyzed and led to the following conclusions.

1) The proposed systematic classification and multitype fusion method accurately implemented the classification and modeling of different reservoirs with matrix pores, vugs, and natural fractures.
2) Fractured-vuggy gas reservoirs were dominated by high-angle structural and horizontal fractures. The DFN model was used to construct different types of natural fractures. This model accurately described the distribution of natural fractures in the internal space of the reservoir and reflected the strong heterogeneity of fractured-vuggy gas reservoirs.
3) The heterogeneity and dynamic water invasion charac-

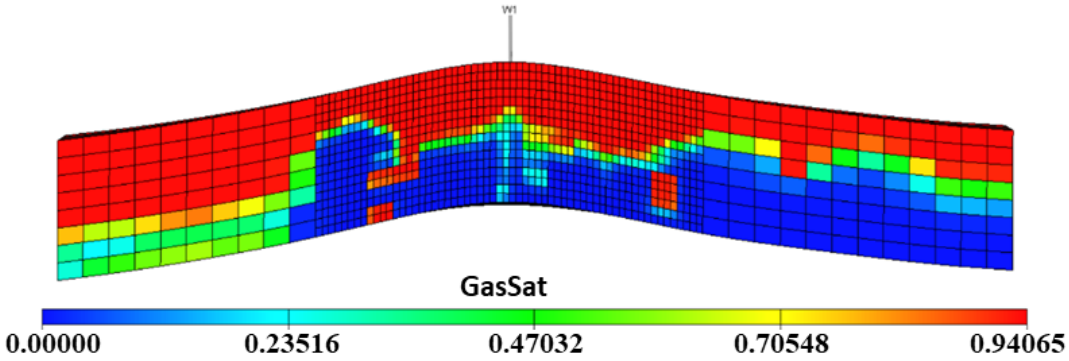


**Fig. 15.** Water saturation during the dynamic process of bottom-water invasion (profile map).

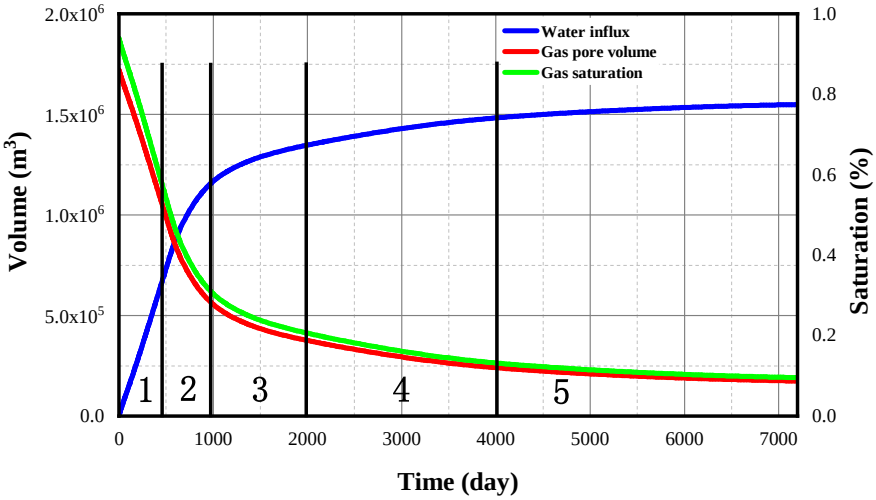


**Fig. 16.** Changes in edge-water influx over time.

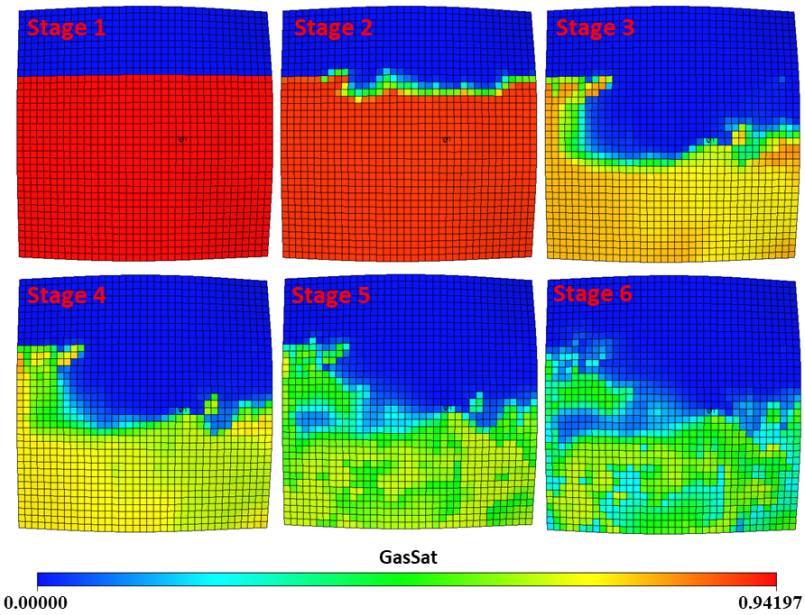


**Fig. 17.** Variations in water saturation during edge-water invasion.

teristics of bottom gas reservoirs were well-described by the grid around the NWM infill well in the simulation. The water at the bottom of the wedge zone flowed along the fracture vertically, and the water cone features were obvious.

4) According to the stages characteristic of edge-water invasion, water flux increased rapidly with time before stage 3. Contrarily, water flux increased slowly with time after stage 3.

## Acknowledgement

This research was supported by the Science and Technology Cooperation Project of the CNPC-SWPU Innovation Alliance (No. 2020CX010402) and the Sichuan Science and Technology Project (No. 2020YFSY0031).

## Conflict of interest

The authors declare no competing interest.



## References

Akbarifard, M. G., Azdarpour, A., Aboosadi, Z. A., et al. Numerical simulation of water production process and spontaneous imbibition in a fractured gas reservoir-A case study on homa gas field. Journal Natural Gas Science and Engineering, 2020, 83: 103603.

Espinola-Gonzalez, O., Guzman-Arevalo, J. D., Ramirez-Cuacenetl, J. R., et al. Evaluation of exploitation strategies for gas reservoirs with water influx in the Miocene formation of the Veracruz Basin through numerical simulation to optimise the recovery factor. Paper SPE 180777 Presented at SPE Trinidad and Tobago Section Energy Resources Conference, Port at Spain, Trinidad and Tobago, 13-15 June, 2016.

Fan, M., Dalton, L. E., McClure, J., et al. Comprehensive study of the interactions between the critical dimensionless numbers associated with multiphase flow in 3D porous media. Fuel, 2019, 252: 522-533.

Golparvar, A., Zhou, Y., Wu, K., et al. A comprehensive review of pore scale modeling methodologies for multiphase flow in porous media. Advances in Geo-Energy Research, 2018, 2(4): 418-440.

Gomes, J. S., Ribeiro, M. T., Deeb, M. E., et al. Lessons learned from static reservoir modelling on complex carbonate fields, onshore UAE. Paper SPE 88780 Presented at Abu Dhabi International Conference and Exhibition, Abu Dhabi, United Arab Emirates, 10-13 October, 2004.

Kossack, C. A. Simulation of gas/oil displacements in vuggy and fractured reservoirs. Paper SPE 101674 Presented at SPE Annual Technical Conference and Exhibition, San Antonio, Texas, 24-27 September, 2006.

Li, X., Fu, X., Tian, J., et al. Heterogeneities of seepage pore and fracture of high volatile bituminous coal core: Implications on water invasion degree. Journal Petroleum Science and Engineering, 2019, 183: 106409.

Lyu, X., Liu, Z., Hou, J., et al. Mechanism and influencing factors of EOR by $N_2$ injection in fractured-vuggy carbonate reservoirs. Journal Natural Gas Science and Engineering, 2017, 40: 226-235.

Ni, G., Cheng, W., Lin, B., et al. Experimental study on removing water blocking effect (WBE) from two aspects of the pore negative pressure and surfactants. Journal Natural Gas Science and Engineering, 2016, 31: 596-602.

Wang, B., Liu, X., Sima, L. Grading evaluation and prediction of fracture-cavity reservoirs in Cambrian Longwangmiao Formation of Moxi area, Sichuan Basin, SW China. Petroleum Exploration and Development, 2019a, 46(2): 301-313.

Wang, J., Zhao, W., Liu, H., et al. Inter-well interferences and their influencing factors during water flooding in fractured-vuggy carbonate reservoirs. Petroleum Exploration Development, 2020, 47(5): 1062-1073.

Wang, Y., Hou, J., Tang, Y., et al. Effect of vug filling on oil-displacement efficiency in carbonate fractured-vuggy reservoir by natural bottom-water drive: A conceptual model experiment. Journal Petroleum Science and Engineering, 2019b, 174: 1113-1126.

Wu, Y.-S., Yuan, D., Kang, Z., et al. A multiple-continuum model for simulating single-phase and multiphase flow in naturally fractured vuggy reservoirs. Journal Petroleum Science and Engineering, 2011, 78(1): 13-22.

Xu, Z., Zhou, X., Zhang, X., et al. Pore-scale investigation on the thermochemical process in uniform and gradient porous media considering immiscible phase. International Communications in Heat Mass Transfer, 2020, 116: 104725.

Yuan, C., Pu, W., Jin, F., et al. Performance of oil-based cement slurry as a selective water-plugging agent in high-temperature and high-salinity cave-fractured carbonate reservoirs. Industrial & Engineering Chemistry Research, 2014, 53(14): 6137-6149.

Zhang, L.-H., Feng, G.-Q., Li, X.-P., et al. Water break through simulation in naturally fractured gas reservoirs with water drive. Journal of Hydrodynamics, 2005, 17(4): 466-472.

Zhou, X., Xu, Z., Xia, Y., et al. Pore-scale investigation on reactive flow in porous media with immiscible phase using lattice Boltzmann method. Journal Petroleum Science and Engineering, 2020, 191: 107224.